

PROCEEDINGS OF SPIE

SPIDigitalLibrary.org/conference-proceedings-of-spie

Polarization-dependent metasurfaces for 2D/3D switchable displays

Zhujun Shi, Federico Capasso

Zhujun Shi, Federico Capasso, "Polarization-dependent metasurfaces for 2D/3D switchable displays," Proc. SPIE 10676, Digital Optics for Immersive Displays, 1067618 (21 May 2018); doi: 10.1117/12.2315658

SPIE.

Event: SPIE Photonics Europe, 2018, Strasbourg, France

Polarization-dependent metasurfaces for 2D/3D switchable displays

Zhujun Shi^a, Federico Capasso^{b*}

^aDepartment of Physics, Harvard University, Cambridge, MA, USA 02138; ^bJohn A. Paulson School of Engineering and Applied Sciences, Harvard University, Cambridge, MA, USA 02138

*Corresponding author: capasso@seas.harvard.edu

ABSTRACT

We proposed a 2D/3D switchable display design based on polarization-dependent metasurfaces. Metasurfaces are ultrathin planar optical devices patterned with subwavelength nanostructures. We design the metasurfaces such that they can simultaneously deflect right-hand circularly polarized (RCP) light to an angle and transmit left-hand circularly polarized (LCP) light to the normal direction. Combined with an active polarization rotator, the device can be switched between high resolution 2D display mode and multiview 3D display mode. Proof-of-principle metasurface designs are demonstrated. The far field radiation patterns in the 2D and 3D mode are simulated and analyzed. The effects of spectral bandwidth and beam directionality are also discussed. Compared with liquid crystal lenses, which is the key element in previous 2D/3D switchable displays, metasurfaces 1) deliver more precise phase profile control, thus less aberrations and higher image quality; 2) offer additional degrees of freedom in polarization manipulation; and 3) can be adapted to much smaller sizes.

Keywords: 2D/3D switchable display, metasurface

1. INTRODUCTION

Three-dimensional (3D) display has attracted great attention lately. Despite the rapid advancement of display technology, conventional two dimensional (2D) display devices can show only flat images without providing depth information. To more vividly present the physical world around us, 3D displays are highly desirable. 3D displays provide not only depth information and spatial relationships, which is usually ambiguous when projected to 2D, but also an immersive viewing experience and more intuitive user interaction.

Recently, stereoscopic 3D displays, which require the audience to wear specialized eyeglasses, have been widely commercialized. However, glass-free autostereoscopic 3D displays remain a technological challenge. Several approaches have been proposed to realize autostereoscopic 3D displays, including holographic 3D, volumetric 3D and multiview 3D¹. Compared to the first two approaches, which require fundamental redesign of the display units, multiview 3D can be readily adapted from the current 2D display technology and has been considered as the most likely candidate for future 3D displays. Multiview 3D displays create 3D images by projecting multiple 2D views corresponding to different observation angles. In practice, the pixels corresponding to different perspective angles are usually multiplexed spatially on the display panel. For a fixed pixel density, this leads to reduced 3D image resolution (inversely proportional to the number of views). In addition, the available 3D content is in shortage compared with the abundant 2D content. These challenges limit the application of 3D-only displays. To address these issues, it is highly desirable to have a 2D/3D switchable display, which can be switched electrically between two working modes - high resolution 2D display mode and low resolution 3D display mode. In this way, one can enjoy the benefits of 3D displays without sacrificing the resolution of 2D images.

Most current 2D/3D switchable display designs fall into three categories (Fig. 1): parallax barrier-based design², active liquid crystal lens (LC lens) based design³, and passive liquid crystal lens based design⁴. The parallax barrier based design (Fig. 1(a)) is comprised of liquid crystal strips that can either directly transmit light (2D mode) or function as alternate transmissive and opaque columns (3D mode), allowing only the light corresponding to the particular viewing zone to be transmitted. This greatly reduces the overall transmittance since at least half of the light is blocked in the 3D mode. In the second approach (Fig. 1(b)), the LC lenses can be electrically controlled to modulate the transmitted light of image pixels. In the OFF state (2D mode), the liquid crystal layer is transparent, allowing light to directly pass through. In the ON state (3D mode), the device functions as a focusing lens. Depending on the relative position of the underlying pixels with respect

to the LC lens center, the transmitted light will be directed to different angles, creating a multiview 3D image. The third approach (Fig. 1(c)) replaces the active LC lenses with passive polarization dependent LC lenses and polarization rotators (e.g. active twisted nematic (TN) cells). The LC lenses are UV cured to maintain a fixed phase retardation profile. The birefringence of liquid crystal allows ordinary rays to directly pass through and extraordinary rays to be focused. The TN polarization rotator, combined with a linear polarizer, can dynamically tune the polarization of the light incident on the passive LC lenses, thus switching between the 2D and 3D mode. Compared to the active LC lens-based design, this approach requires no dynamic tuning of the spatial phase retardation profile and the TN cells used can be directly adapted from LCD panels.

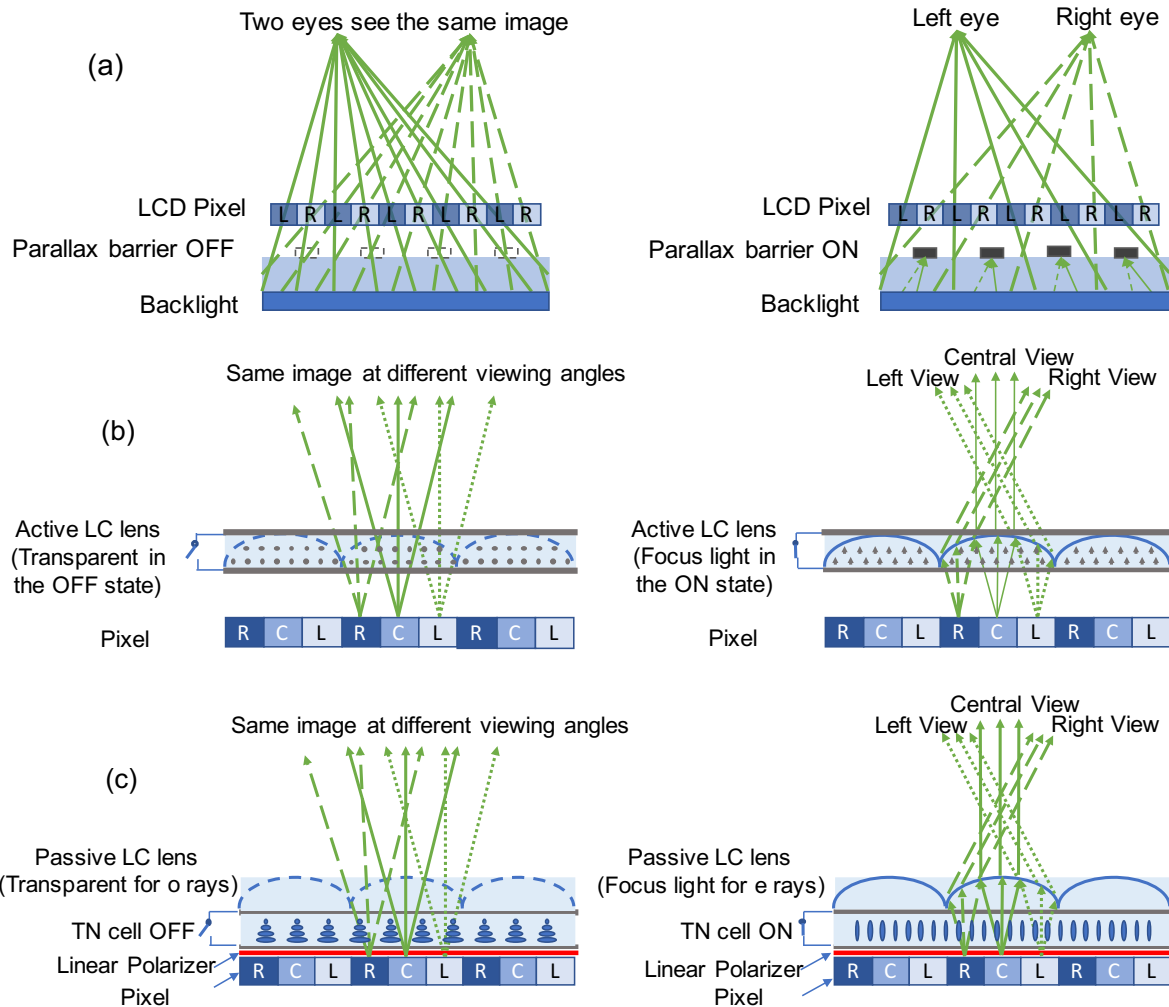


Figure 1. (a) Parallax barrier-based 2D/3D switchable display. Left: 2D mode. Right: 3D mode. (b) Active LC lens-based 2D/3D switchable display. Left: 2D mode. Right: 3D mode. (c) Passive LC lens-based 2D/3D switchable display. Left: 2D mode. Right: 3D mode.

Despite their various implementations, the previously demonstrated 2D/3D switchable displays all rely on the liquid crystal modules (LC parallax barriers, active/passive LC lenses) to generate multiple views. Although a well-established technology, the use of liquid crystal modules, especially the LC lenses, has several drawbacks/limitations in this application. First, it is very challenging to control precisely the phase retardation profile of LC lenses. In general, LC lenses suffer from poor focusing ability, undesired optical aberrations and serious crosstalk, even with sophisticated electrode patterning. For active LC lenses, the large driving electric voltage required can also be a concern. Second, the size of LC lenses limits the 3D image resolution. With the advances in display manufacturing, it is expected that the pixel size will consistently decrease over years. Smaller size of individual pixels leads to increased 2D image resolution. However, the

3D image resolution is still dictated by the ‘multiview pixel’ size – in this case the LC lens diameter, which is usually on the order of hundreds of micrometers. Third, the 2D and 3D modes are limited to operate at linear polarizations. In many situations, however, it is desired to have circularly polarized light. For example, people usually use a linear polarizer and a quarter waveplate rotated by 45° to remove the ambient light reflected from the display panel. In this case, linearly polarized light is converted to circularly polarized light after passing through the quarter waveplate, and only half of the light can transmit through the final polarizer. Notice that this cannot be circumvented by introducing another waveplate or polarization rotator in between to transform the linearly polarized light to circularly polarized light, as this will fail to block the back reflected ambient light. If the light incident on the quarter waveplate is of a certain circular polarization, however, light can pass through without significant loss of efficiency.

To break away from these limitations, we propose a novel 2D/3D switchable display design based on metasurfaces – ultrathin planar optical devices patterned with subwavelength nanostructures⁵. With proper engineering of the nanostructures, metasurfaces can offer precise and complete control over the phase, transmittance and the polarization of the transmitted light, beyond the scope of conventional refractive and diffractive optics. One unique property of metasurfaces is the ability to implement distinct phase profiles for an arbitrary pair of orthogonal polarizations (polarization-dependent metasurfaces)⁶. In this paper, we design the metasurfaces such that it can simultaneously deflect right-hand circularly polarized (RCP) light to an angle (Fig. 2(a)) and transmit left-hand circularly polarized (LCP) light to the normal direction (Fig. 2(b)) When combined with an active polarization rotator, such as TN cells, the device can switch between the high resolution 2D display mode and the multiview 3D display mode. Compared with the previous designs, our metasurface based approach has several advantages:

- 1) Metasurfaces offer precise control over the phase profile simultaneously at two polarizations, reducing aberrations and crosstalk. This improves the overall image quality.
- 2) Metasurfaces can be adapted to arbitrary sizes, as small as $5\ \mu\text{m}$ or as large as hundreds of micrometers. This enables potential high resolution 3D displays.
- 3) Metasurfaces can be designed for an arbitrary pair of orthogonal polarizations, in particular, circular polarizations. Therefore, they are compatible with back-reflection removal components, and other polarization control components.
- 4) Metasurfaces are ultrathin, and lightweight.

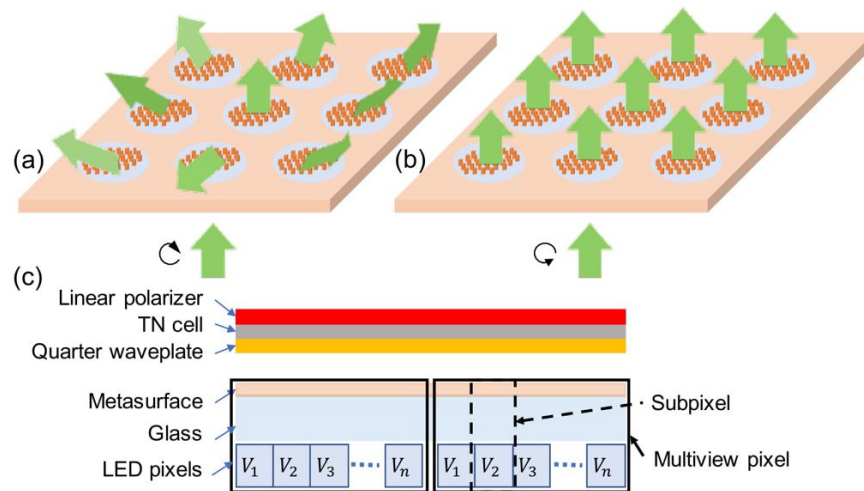


Figure 2. Schematic of a metasurface-based multiview pixel. Each patch of metasurface corresponds to one subpixel that projects light to a specific viewing angle in the 3D mode. Several subpixels are bundled together to form a multiview pixel. (a) 3D mode: For RCP incident light, the metasurfaces diffract light to the designed viewing angle corresponding to the first diffraction order. (b) 2D mode: For LCP incident light, the metasurfaces transmit light to the normal direction. (c) Side view of the structure. The metasurface layer is patterned on a glass substrate above the LED pixels. $V_1 \dots V_n$ refers to different subpixels. The linear polarizer and quarter waveplate are used to remove back reflection from the ambient light. The TN cell is used as an active polarization rotator, which rotates the linear polarization by 90° in the OFF state, and maintains the polarization in the ON state.

2. WORKING PRINCIPLE

To incorporate multiple views, several subpixels, each corresponding to a different viewing angle, are bundled together to form a multiview pixel (Fig. 2(a)-(b)). The number of subpixels equals the number of views in the 3D mode. The side-view of the device is shown in Figure 2(c). Each metasurface is placed above its underlying LED pixel, with a layer of transparent spacer (glass) in between. In this design, we also consider a back-reflection removal component consisting of a linear polarizer and a quarter waveplate. An active polarization rotator (TN cells) is placed between the passive linear polarizer and the quarter waveplate. By turning on and off the TN cells, the device can be switched between the 3D and 2D operating mode. Note that here the liquid crystal layer is only used to modulate the final polarization, not to provide multiple views. It is uniformly turned on and off, requiring no active or passive local modulation of refractive index. Therefore, it does not suffer from the previously mentioned drawbacks of LC lens-based 2D/3D switchable displays.

The bandwidth and directionality of the emitted light plays an important role in the design. Since in the 3D mode the metasurfaces are essentially blazed gratings, the final diffracted angle is a function of both the incident angle and the wavelength. Finite bandwidth and divergence lead to broadening of the diffracted beam in the far field. Ideally, the divergence angle ($\Delta\theta$) of the diffracted beam should be large enough to allow for smooth transition between neighboring views, but not too large to avoid excessive overlapping and crosstalk⁷. Therefore, the angular separation between neighboring views ($\Delta\phi$) should be comparable to $\Delta\theta$. For a given field of view (FOV) and diffracted beam divergence angle ($\Delta\theta$), the achievable number of views is proportional to $\left(\frac{\text{FOV}}{\Delta\theta}\right)^2$. To accommodate more number of views in the 3D mode, it is desirable to design the light emitting elements to have higher directionality. This can be achieved by adding additional optical cavities or engineering the existing optical cavities in the LEDs⁸. In the 2D mode, however, high directionality is usually unwanted, as it limits the viewing zone of the 2D images. To address this contradiction, we design the metasurfaces to function as a concave (diverging) lens, rather than a uniform transparent layer, in the 2D mode. In this way, relatively high directionality (required for more number of views) in the 3D mode and low directionality (required for broader viewing zone) in the 2D mode can be achieved at the same time.

The working principle is illustrated in Figure 3. The emitted light from the LEDs is unpolarized, consisting of half LCP and half RCP light. The metasurface functions as a diverging lens for LCP light, and as a blazed grating for RCP light. Note that in addition to deflect or transmit the beam, the metasurface also converts LCP to RCP and vice versa (more detailed discussion can be found in the theory section). The quarter waveplate then transforms the LCP and RCP light to x and y linearly polarized light. In the OFF state, the TN cell rotates linear polarization by 90°. The passive linear polarizer is oriented such that only the x polarization, which corresponds to the 2D image, passes through. In the ON state, the TN cell is transparent, and there is no polarization rotation. In this case, the x polarization corresponds to the 3D image.

The metasurfaces can be fabricated via single-step lithography using the method described in ref 9⁹. The center of the metasurface and that of the corresponding subpixel do not need to be precisely aligned, but for best result one metasurface should cover only one subpixel and should not overlap with other subpixels.

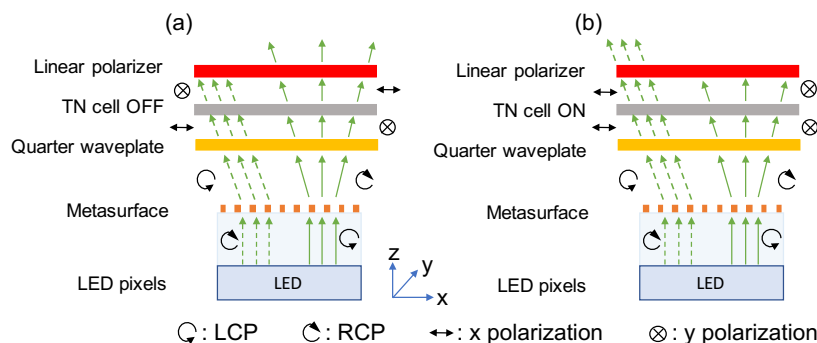


Figure 3. Working principle of the metasurface-based 2D/3D switchable display. (a) 2D mode. (b) 3D mode.

3. THEORY

3.1 Polarization optics in metasurfaces

Figure 4(a) shows the schematic of the metasurfaces' building blocks - rectangular TiO₂ nanopillar patterned on top of a glass substrate. The height of the nanopillars (H) is kept constant across the metasurface for easier fabrication. The width (W) and length (L) of the nanopillars can be varied locally. Physically, the nanopillars can be approximated as truncated waveguides. Light gains a phase shift after passing through the nanopillars, proportional to the effective index of the truncated waveguide and the propagation length (Eqn. 1). The rectangular cross-sectional shape in general leads to different effective indices for x and y polarized light, the so-called form birefringence.

$$\phi_x = \frac{2\pi}{\lambda} n_{eff,x} H \quad \phi_y = \frac{2\pi}{\lambda} n_{eff,y} H \quad (1)$$

We can characterize the nanopillar by its Jones matrix T , which relate the phase and polarization ellipse of the incident and transmitted light by $E_{transmitted} = TE_{incident}$. The Jones matrix in its eigenbasis, T_0 , is diagonal (Eqn. 2). Here ϕ_x and ϕ_y are the phase shift along x and y axis; t_x and t_y are the transmittance respectively. In our design, t_x and t_y are similar, and can be factored out of the matrix as an overall transmittance t .

$$T_0 = \begin{pmatrix} t_x e^{i\phi_x} & 0 \\ 0 & t_y e^{i\phi_y} \end{pmatrix} \cong t \begin{pmatrix} e^{i\phi_x} & 0 \\ 0 & e^{i\phi_y} \end{pmatrix} \quad (2)$$

In general, the nanopillars can be rotated by an angle θ (Fig. 4(b)), introducing an additional geometrical phase shift (Eqn. 3). Here $R(\theta)$ is the 2D rotation matrix.

$$T(\theta) = R(-\theta)T_0R(\theta) \quad (3)$$

For right-handed and left-handed circularly polarized incident light, denoted by σ^+ and σ^- respectively, the transmitted light is given by

$$T(\theta)\sigma^+ = te^{\frac{i(\phi_x+\phi_y)}{2}} \left\{ \cos^2 \frac{\phi_x-\phi_y}{2} \sigma^+ + e^{2i\theta} \sin^2 \frac{\phi_x-\phi_y}{2} \sigma^- \right\} \quad (4)$$

$$T(\theta)\sigma^- = te^{\frac{i(\phi_x+\phi_y)}{2}} \left\{ \cos^2 \frac{\phi_x-\phi_y}{2} \sigma^- + e^{-2i\theta} \sin^2 \frac{\phi_x-\phi_y}{2} \sigma^+ \right\} \quad (5)$$

If $\phi_x - \phi_y = \pm\pi$, the above expression can be further simplified as

$$T\sigma^+ = te^{i\left[\frac{(\phi_x+\phi_y)}{2}+2\theta\right]}\sigma^- \quad (6)$$

$$T\sigma^- = te^{i\left[\frac{(\phi_x+\phi_y)}{2}-2\theta\right]}\sigma^+ \quad (7)$$

The transmitted light is converted to its orthogonal polarization (RCP to LCP, and vice versa). The phase shift consists of two parts: a propagation phase term $\phi_{prop} = \frac{(\phi_x+\phi_y)}{2}$ that is common to both polarizations, and a geometrical phase term $\phi_{geo} = \pm 2\theta$ whose sign is opposite for RCP and LCP. By tuning ϕ_{prop} and ϕ_{geo} , the phase shift for RCP and LCP can be controlled independently.

3.2 Metasurface design

The metasurface functions as a concave lens in the 2D mode. The required phase profile is given by

$$\phi_{LCP}(X, Y) = \frac{2\pi}{\lambda} (\sqrt{f^2 + X^2 + Y^2} - f) \quad (7)$$

where $f = \sqrt{X^2 + Y^2} / \tan \alpha$, α is the target half angle (Fig. 5), X, Y is the location on the metasurface.

The metasurface functions as a blazed grating in the 3D mode. The required phase profile is given by

$$\phi_{RCP}(X) = \frac{2\pi}{\lambda} X \sin \beta \quad (8)$$

where β is the target deflection angle (Fig. 5).

According to Eqn. 6-7, we can back calculate the required propagation phase and rotation angle.

$$\phi_{prop} = (\phi_{RCP} + \phi_{LCP})/2 \quad (9)$$

$$\theta = (\phi_{RCP} - \phi_{LCP})/4 \quad (10)$$

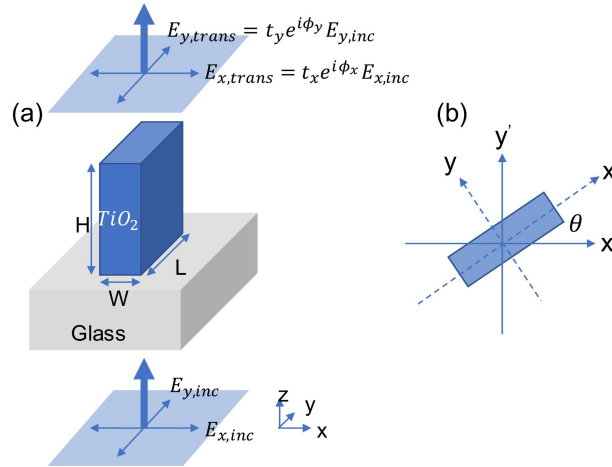


Figure 4. (a) Schematic of the metasurfaces' building blocks - rectangular TiO₂ nanopillar patterned on top of a glass substrate. The x, y polarized light will gain a phase shift of ϕ_x and ϕ_y after passing through the nanopillars. t_x and t_y are the transmittance along x and y axis respectively. (b) Top view of a rotated nanopillar.

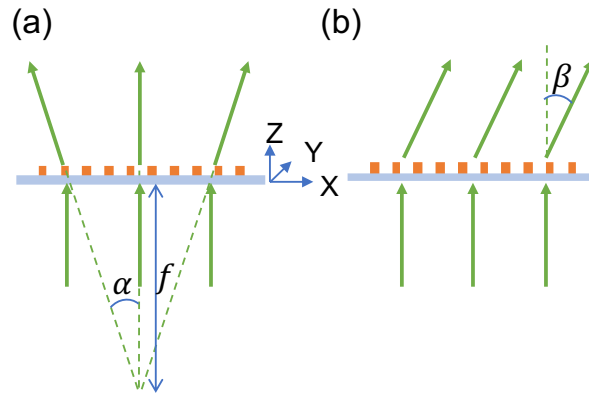


Figure 5. Ray diagrams. (a) 2D mode. (b) 3D mode.

4. RESULTS

We simulated individual nanopillar's transmittance and phase shift using finite difference time domain method. The nanopillar height (H) is fixed to be $1\mu\text{m}$. The pillars' center-to-center distance is 350 nm . The pillar width and length is varied between 50 to 300 nm . In the design, we choose the nanopillars whose conversion efficiency is above 85% .

Four different metasurfaces are designed to deflect the beam to $\beta = 0^\circ, 10^\circ, 20^\circ, 30^\circ$ in the 3D mode respectively. In all designs, the half diverging angle in the 2D mode is fixed to be $\alpha = 20^\circ$. Viewing angles of $\beta = -10^\circ, -20^\circ, -30^\circ$ can be achieved by simply patterning the metasurfaces in a mirror reflection manner.

To prove the effectiveness of our phase design method, we compare the required (blue solid lines) and realized (red circles) phase profile (Fig. 6). At each location (X, Y) on the metasurface, we assign a specific nanopillar that minimizes the phase error. The realized phase profile matches well with the required one.

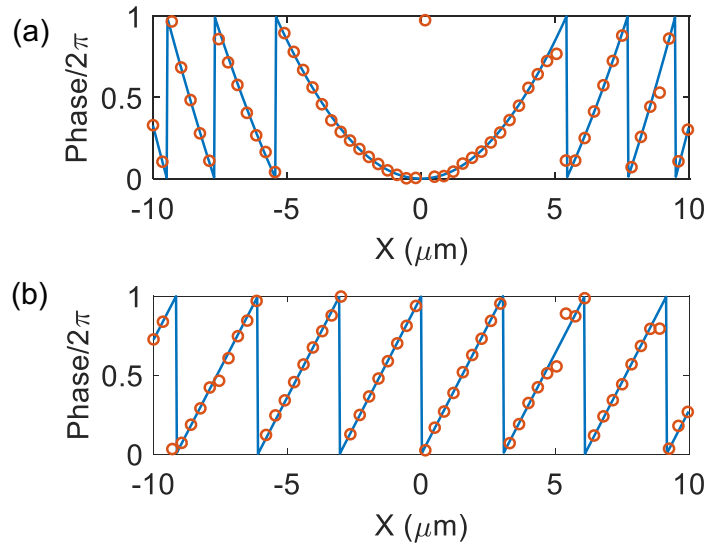


Figure 6. Required and realized phase profiles along the X axis. The metasurface is designed to have a half diverging angle of $\alpha = 20^\circ$ in the 2D mode, and a deflection angle of $\beta = 10^\circ$. (a) Blue solid line: required phase profile for LCP; red circles: realized phase profile for LCP. The hyperbolic phase profile corresponds to a concave lens. (b) Blue solid line: required phase profile for RCP; red circles: realized phase profile for RCP. The linear phase profile corresponds to a blaze grating (beam deflector).

We also did full wave simulations of the metasurfaces. The diameter of the metasurfaces is designed to be $20 \mu\text{m}$. The incident wavelength is centered at 530 nm , with a FWHM spectral bandwidth of 10 nm .

Figure 7(a)-(b) show the far field radiation pattern for LCP and RCP incident light respectively. Here we assume the incident beam has a divergence angle of 5° . For LCP (2D mode), light is transmitted to the zeroth order. The beam divergence angle is broadened to 35° due to the concave lens phase profile implemented (Fig. 7(a)). For RCP (3D mode), light is deflected to the $+1^{\text{st}}$ order (Fig. 7(b)) with an average efficiency of 83% . The 0^{th} , -1^{st} and higher diffraction orders are negligible in our designs thanks to the precise control of phase profiles enabled by metasurfaces. The divergence angle of the deflected beam ($\Delta\theta$) is about 9° , providing a smooth transition between the neighboring views (angular separation $\Delta\phi = 10^\circ$ by design) while avoiding excessive overlapping and crosstalk.

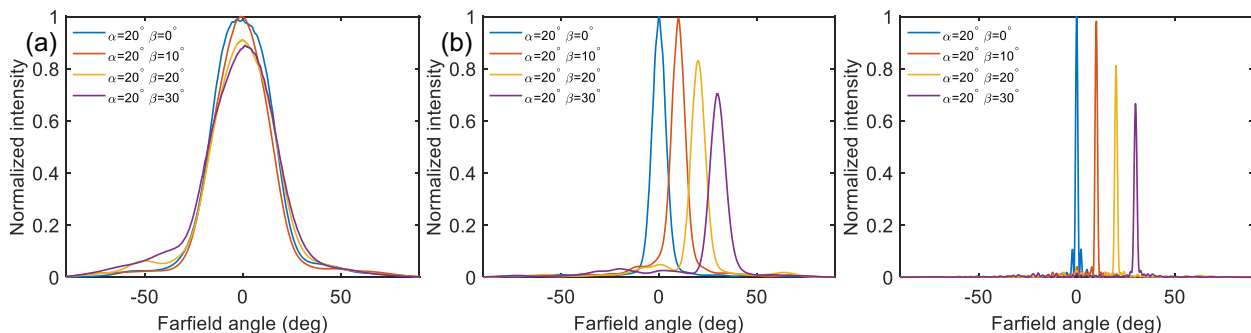


Figure 7. (a) Normalized intensity distribution in the farfield for LCP. The incident light has a FWHM spectral bandwidth of 10 nm , and divergence angle of 5° . (b) Normalized intensity distribution in the farfield for RCP incident light. The incident light has a FWHM spectral bandwidth of 10 nm , and divergence angle of 5° . (c) Normalized intensity distribution in the farfield for RCP incident light. The incident light is collimated and has a FWHM spectral bandwidth of 10 nm .

Figure 7(c) shows the far field radiation pattern for the same metasurface designs but with collimated incident light. The FWHM spectral bandwidth is again taken to be 10 nm . Compared with Fig.7(b), one can see that the divergence of the deflected beam is primarily dominated by the divergence of the incident light. If highly directional emitted light can be achieved, one can further increase the number of views to enhance the 3D effect.

5. SUMMARY

We present a 2D/3D switchable display design based on polarization-dependent metasurfaces. By imparting a concave lens phase profile for LCP, and a blazed grating phase profile for RCP, the metasurfaces can either generate high resolution 2D images or multiview 3D images. The two modes can be electrically switched using an active polarization rotator. As a proof-of-principle demonstration, we designed a metasurface-based multiview pixel with a target field of view and angular resolution of 60° and 10°, respectively. The angular resolution can be further improved by engineering the directionality of the LEDs.

ACKNOWLEDGEMENT

This research is supported in part by the Air Force Office of Scientific Research (MURI FA9550-14-1-0389 and FA9550-16-1-0156). Z.S. thanks Joon-Suh Park, Haoning Tang and Zhehao Dai for helpful discussion.

REFERENCES

- [1] J. S. Geng, "Three-dimensional display technologies," *Advances in Optics and Photonics*, 5(4), 456-535 (2013).
- [2] W. Mphepo, Y. P. Huang, and H. P. D. Shieh, "Enhancing the Brightness of Parallax Barrier Based 3D Flat Panel Mobile Displays Without Compromising Power Consumption," *Journal of Display Technology*, 6(2), 60-64 (2010).
- [3] T. Dekker, S. T. de Zwart, O. H. Willemsen *et al.*, "2D/3D switchable displays," *Liquid Crystal Materials, Devices, and Applications Xi*, 6135, (2006).
- [4] H. Ren, S. Xu, Y. F. Liu *et al.*, "Switchable focus using a polymeric lenticular microlens array and a polarization rotator," *Optics Express*, 21(7), 7916-7925 (2013).
- [5] N. F. Yu, and F. Capasso, "Flat optics with designer metasurfaces," *Nature Materials*, 13(2), 139-150 (2014).
- [6] J. P. B. Mueller, N. A. Rubin, R. C. Devlin *et al.*, "Metasurface Polarization Optics: Independent Phase Control of Arbitrary Orthogonal States of Polarization," *Physical Review Letters*, 118(11), 113901 (2017).
- [7] D. Fattal, Z. Peng, T. Tran *et al.*, "A multi-directional backlight for a wide-angle, glasses-free three-dimensional display," *Nature*, 495(7441), 348-351 (2013).
- [8] T. Tsutsui, N. Takada, S. Saito *et al.*, "Sharply Directed Emission in Organic Electroluminescent Diodes with an Optical-Microcavity Structure," *Applied Physics Letters*, 65(15), 1868-1870 (1994).
- [9] R. C. Devlin, M. Khorasaninejad, W. T. Chen *et al.*, "Broadband high-efficiency dielectric metasurfaces for the visible spectrum," *Proceedings of the National Academy of Sciences of the United States of America*, 113(38), 10473-10478 (2016).